This article has been accepted for publication in a future issue of this journal, but has not been fully edited. Content may change prior to final publication. Citation information: DOI 10.1109/JSTARS.2021.3087742, IEEE Journal of Selected Topics in Applied Earth Observations and Remote Sensing

Scatterometer Sea Surface Wind Product Validation for HY-2C

Zhixiong Wang, Juhong Zou, Ad Stoffelen, Wenming Lin, Anton Verhoef, Xiuzhong Li, Yijun He, Youguang Zhang, Mingsen Lin

***Abstract*—The Chinese HY-2C satellite was launched on Sep. 21, 2020, carrying the new Ku-band scatterometer (HSCAT-C). Different from the other currently operating scatterometers, the HSCAT-C is in a non-sun-synchronous orbit and as such it will be useful for the cross-calibration of sea surface wind products from current space-borne scatterometers and radiometers. In this study, the HSCAT-C wind products are validated by comparing to collocated winds from buoys, ECMWF model, and several other scatterometers. The results show that the quality of HSCAT-C winds is very good: in comparison with buoy winds, the wind speed standard deviation (SD) and direction root-mean-square error (RMSE) are 1.03 m/s and 15.9° respectively. The HSCAT-C winds show very good agreements with the HSCAT-B winds, especially in the range of [4, 17] m/s. In addition, as HSCAT-C is a rotating pencil-beam scatterometer, some common error characteristics are also clearly found in the wind products. Based on the validation results and existing scatterometer application experience, it is believed that the availability of the HSCAT-C wind product would greatly benefit the scientific and user community.**

***Index Terms*—Radar measurements, sea surface, spaceborne radar, wind.**

I. Introduction

THE scatterometer onboard the Chinese HY-2C satellite (HSCAT-C) was launched on Sep. 21, 2020. The operation of the HSCAT-C greatly improves the temporal and spatial sampling of the global sea surface winds by satellite scatterometers. This manuscript aims to give a view on the quality of the HSCAT-C wind products.

HSCAT-C is an instrument identical to the scatterometer (HSCAT-B) onboard the HY-2B satellite. However, the HY-2B and HY-2C satellites are flying in very different orbits. The HY-2B is in a sun-synchronous orbit with 99.34° inclination and it crosses the equator at nearly the same local solar time (LST) every day (Descending at 6 AM, Ascending at 6 PM UTC) [1], whereas the HY-2C is in a non-sun-synchronous orbit with 66.0° inclination and its equator crossing time is shifting each orbit. As such, the HSCAT-C can generate a large number of closely collocated winds with other operating scatterometers and microwave radiometers. The HSCAT-C measurement swath reaches a maximum latitude of about 74° N and 74° S. The processing and distribution of HSCAT data are operated by the Chinese National Satellite Ocean Application Service (NSOAS).

In addition to the HSCAT-C and HSCAT-B scatterometers, the following five scatterometers are also operating now: the Advanced scatterometer (ASCAT) onboard the MetOp-A, MetOp-B, and MetOp-C satellites, the OSCAT2 scatterometer onboard the SATSAT-1 satellite, and the scatterometer onboard the China-France Oceanography Satellite (CFOSAT). All these scatterometers operate at either C-band or Ku-band. The ASCAT operates at C-band and uses fixed-beam antennas, but the others operate at Ku-band and use rotating-beam antennas. All these scatterometers together can be regarded as a virtual constellation for ocean surface vector wind (OSVW-VC). Although the current OSVW-VC is not in an optimized design in terms of temporal sampling, the situation is improving with closer international coordination [2]. On the other hand, it is important to notice that inconsistencies in scatterometer wind products do exist, especially between C- and Ku-band systems. Nevertheless, almost all existing scatterometers can provide overall good retrievals of sea surface wind speed and direction (equivalent to 10 m height). For instance, several studies show that all the standard deviation (SD) of wind speed and root mean square (RMS) of wind direction between HSCAT-B, ASCAT-C, or OSCAT2 winds and buoy winds are within 1.1 m/s and 19° respectively [3-5].

In validating scatterometer wind products, the following five methodologies are generally used.

This work was supported in part by the National Key R&D Program of China under Grant 2019YFD0901402, in part by the National Natural Science Foundation of China under Grant 41906153, Grant 41706197 and Grant 41706202, in part by the International Cooperation Project of the National Natural Science Foundation of China under Grant 41620104003, and in part by EUMETSAT OSI SAF. (Corresponding authors: Juhong Zou; Zhixiong Wang.)

Z. Wang is with the School of Marine Sciences, Nanjing University of Information Science and Technology, Nanjing 210044, China, and also with the Laboratory for Regional Oceanography and Numerical Modeling, Qingdao National Laboratory for Marine Science and Technology, Qingdao 266000, China (e-mail: wangzhixiongcn@163.com).

J. Zou and Y. Zhang are with the Key Laboratory of Space Ocean Remote Sensing and Application, Ministry of Natural Resources, Beijing 100081, China, also with the National Satellite Ocean Application Service, Beijing 100081, China, and also with the Southern Marine Science and Engineering Guangdong Laboratory, Guangzhou 511458, China (e-mail: zoujuhong@mail.nsoas.org.cn; zhangyouguang@mail.nsoas.org.cn).

M. Lin is with the Key Laboratory of Space Ocean Remote Sensing and Application, Ministry of Natural Resources, Beijing 100081, China, also with the National Satellite Ocean Application Service, Beijing 100081, China (e-mail: mslin@mail.nsoas.org.cn).

W. Lin, X. Li, and Y. He are with the School of Marine Sciences, Nanjing University of Information Science and Technology, Nanjing 210044, China (e-mail: wenminglin@nuist.edu.cn; lixiuzhong@nuist.edu.cn; yjhe@nuist.edu.cn).

A. Stoffelen and A. Verhoef are with the Royal Netherlands Meteorological Institute, 3730 AE De Bilt, The Netherlands (e-mail: ad.stoffelen@knmi.nl; anton.verhoef@knmi.nl).

Comparison with buoy winds: Anemometers on buoy stations can provide in situ time-averaged wind speed and direction, and thus buoy winds are usually used as ground truth in calibrating/validating remote sensing retrievals of sea surface winds. However, the spatial representativeness and sparse geographical locations of buoy data should be carefully considered. Besides, the differences between scatterometer wind and buoy winds show strong seasonal and annual variations [6, 7]. Thus, the same buoy stations and time period are preferable.

Comparison with NWP model winds: Since model data can be matched for each scatterometer wind vector cell (WVC), this method can show error characteristics that are related to scatterometer measuring geometry. For instance, the error characteristics of wind speed and direction in nadir region of the swath are well-known, and can be clearly shown in the plots of wind differences as a function of cross-track index (indicating the location of a WVC across the swath) [8, 9].

Comparison with winds from other space-borne remote sensing sensors: Winds from other scatterometers or microwave radiometers can also be used in comparisons, and such results could reveal systematic difference and further help to improve consistency of remote sensed winds [10-13].

Triple collocation (TC) analysis: The TC method was introduced by Stoffelen in 1998 to overcome problems in dual comparisons, and is now widely used in geophysical data validation [14-16]. The three sources of winds are typically scatterometer, NWP model, and buoy. The triple collocation method can give the measurement errors from the coarse resolution NWP model perspective, from the intermediate resolution scatterometer perspective, or from the fine resolution buoy perspective.

Spatial analysis: Spectral analysis of spatial structures in the scatterometer products is done for detecting noise and assess the relative amount of small-scale information [15].

In addition, the effectiveness of quality control (QC) flags is another important factor and should be considered in validating scatterometer wind products [17]. In this study, we refer to state-of-the-art findings on error attribution, representation and calibration using triple collocation comparison of C-band and Ku-band winds in association with buoy and ECMWF winds in [18].

In section 2 the datasets used in this study will be introduced, including the numerical weather prediction (NWP) model data, several scatterometer wind products (HSCAT-C, HSCAT-B, OSCAT2, ASCAT-B, ASCAT-C), buoy winds, and their collocated data. Section 3 gives the validation results and discussions. Finally, conclusions are presented in Section 4.

II. Datasets

A. NWP Data

In all scatterometer wind retrieval processing, a background wind filed is needed for the wind ambiguity removal. The NWP model winds at 10-m height are favorably used, such as European Centre for Medium-Range Weather Forecasts (ECMWF) model data. Even so, the wind data are available in three different types, i.e., stress-equivalent winds, equivalent neutral winds, and real winds [19]. However, the stress-equivalent winds are not directly available in ECMWF outputs, but can be calculated based on 10-m equivalent neutral winds or 10-m real winds with some auxiliary data. Currently, the ECMWF stress-equivalent winds are used in scatterometer wind processing at Royal Netherlands Meteorological Institute (KNMI), whereas the real winds of ECMWF operational forecasts are used in scatterometer wind processing at NSOAS.

B. NSOAS HSCAT Scatterometer Wind Products

The HSCAT-C and HSCAT-B wind data are produced using the same wind retrieval procedure, which is developed based on the well-known pencil-beam scatterometer wind processor (PenWP v2.2). The PenWP is released by KNMI in the framework of the Satellite Application Facilities on Numerical Weather Prediction (NWPSAF) and Ocean and Sea Ice (OSI SAF), and sponsored by the European Organisation for the Exploitation of Meteorological Satellites (EUMETSAT). In the wind retrieval processing, the NSCAT-4 geophysical model function (GMF) and wind inversion algorithm of the multiple solution scheme (MSS) are used to generate wind ambiguities, and then the two-dimensional variational ambiguity removal (2DVAR) method is used for ambiguity removal. In addition, the HSCAT sea ice screening is done by using the sea ice edge products from the EUMETSAT OSI SAF, and this is very different from the step done by PenWP. Noting that, the HSCAT-B and HSCAT-C wind products are produced using the same procedures, in terms of backscatter calibration, wind inversion, wind ambiguity removal, and quality control.

In this study, the HSCAT-C and HSCAT-B backscatter measurements are calibrated using the method of NWP ocean calibration (NOC), in which the ECMWF real winds over the global oceans are used as inputs. The following calibration coefficients are achieved and used in producing wind products: for HSCAT-B, the value of +0.42 dB and -0.72 dB are added to inner-beam (HH polarized) and outer-beam (VV polarized) measurements respectively; for HSCAT-C, the value of -1.25 dB and -1.39 dB are used for inner-beam and outer-beam measurements respectively.

C. KNMI ASCAT and OSCAT2 Wind Products

The ASCAT-B, ASCAT-C and OSCAT2 near real time (NRT) wind products in binary universal form for the representation of data (BUFR) format are collected from the KNMI ftp site [20, 21]. Although several wind product grid sizes are available, the wind products on the 25-km swath grid are used. These are spatially comparable with HSCAT winds,

This article has been accepted for publication in a future issue of this journal, but has not been fully edited. Content may change prior to final publication. Citation information: DOI 10.1109/JSTARS.2021.3087742, IEEE Journal of Selected Topics in Applied Earth Observations and Remote Sensing

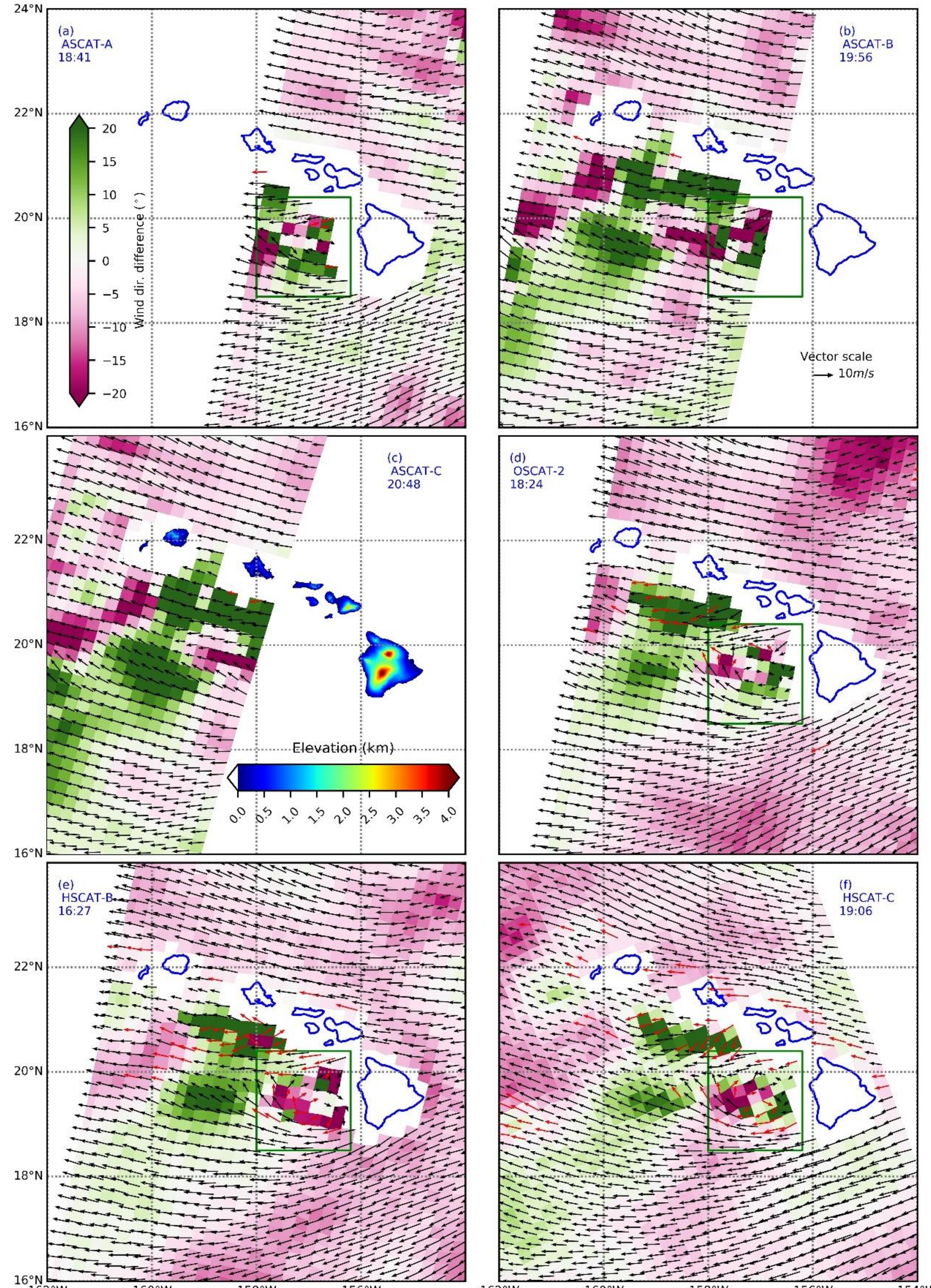

Fig. 1. Wind fields around the Hawaii islands from (a) ASCAT-A, (b) ASCAT-B, (c) ASCAT-C, (d) OSCAT2, (e) HSCAT-B, and (f) HSCAT-C, and their observing time are at about 18:41, 19:56, 20:48, 18:24, 16:27, and 19:06 UTC on Oct. 13, 2020, respectively. The scatterometer wind vectors flagged by QC are shown in red. The length of arrow represents the wind speed of each vector. The background color represents the wind direction differences between scatterometer and their background winds.

thus minimizing spatial match errors. Besides, the CMOD7 GMF is used in ASCAT operational wind processing, and the NSCAT-4 GMF is used in OSCAT2 wind processing. It is interesting to note that the OSCAT2 backscatter measurements do not need compensation for non-linearity above -19 dB (for about 0.1 dB decrease per additional dB), since the switch to redundant hardware in June 2019.

D. Buoy Winds

Buoy winds were obtained from the ECMWF MARS archive,

This article has been accepted for publication in a future issue of this journal, but has not been fully edited. Content may change prior to final publication. Citation information: DOI 10.1109/JSTARS.2021.3087742, IEEE Journal of Selected Topics in Applied Earth Observations and Remote Sensing

TABLE 1
WIND COMPARISONS BETWEEN SCATTEROMETER AND BUOY

SCATTEROMETER WINDS	NUMBER	WIND SPEED		U COMPONENT		V COMPONENT		DIRECTION RMSE
		BIAS(M/S)	SD(M/S)	BIAS(M/S)	SD(M/S)	BIAS(M/S)	SD(M/S)	
HSCAT-C	50 572	-0.14	1.03	-0.13	1.53	-0.02	1.59	15.9°
HSCAT-B	44 198	-0.21	1.00	-0.12	1.51	0.04	1.50	14.8°
OSCAT2	46 194	-0.10	1.05	-0.13	1.59	-0.03	1.55	15.5°
ASCAT-B	25 198	-0.06	0.95	-0.14	1.35	-0.11	1.52	15.7°
ASCAT-C	24 884	-0.08	0.96	-0.15	1.43	-0.10	1.50	16.0°

and we use all buoys that were not blacklisted by ECMWF [22]. The buoy winds are measured hourly by averaging the wind speed and direction over 10 min (from 5 min before the hour to 5 min after). The real winds at a given anemometer height have been converted to 10-m equivalent neutral winds using the Liu-Katsaros-Businger (LKB) model [23].

E. Collocated Datasets

In this study, four months (from Oct. 1, 2020 to Jan. 31 2021) of the following collocated datasets are matched and used: HSCAT-C & HSCAT-B, HSCAT-C & OSCAT2, HSCAT-C & ASCAT-B, HSCAT-C & ASCAT-C, and HSCAT-C & buoy. In all collocation cases, the matching criteria are set as within $25/\sqrt{2}$ km for geographical distance and 30 minutes for temporal difference.

III. VALIDATION RESULTS AND DISCUSSION

A. A Case of Wind Field and QC

The wind fields provided by multiple scatterometers in the area of the Hawaii islands are shown in Fig. 1. In Fig. 1c, the elevations of land (The ASTER Global Digital Elevation Model (GDEM) Version 3, accessed from EARTHDATA) are shown in color. The wind direction differences in the range of [-180, 180] between scatterometer and ECMWF winds are shown as background color. Besides, the scatterometer wind vectors which are flagged by QC are shown in red. Figure 1e, 1d, 1a, 1f, 1b, and 1c show the wind fields measured by HSCAT-B, OSCAT-2, ASCAT-A, HSCAT-C, ASCAT-B, and ASCAT-C at 16:27, 18:24, 18:41, 19:06, 19:56, and 20:48 UTC, respectively.

In Fig. 1, it is interesting to look at the wind flows shown in the green box. They are affected by the Hawaii's Big Island and observed by the different scatterometers over a short time interval. The lee vortices and reverse flow toward Big Island in the lee of the predominate flow are clear in HSCAT-C, HSCAT-B and OSCAT2 winds, and of slightly different shape in the ASCAT winds. Kilpatrick et al. and Hutchings et al. have shown that the lee vortices and reverse flow are expected to exist due the effects of topography [24, 25]. There is a strong wind variability seen in the area of the green box, where only a few wind vectors are flagged in ASCAT wind products. While only a few wind vectors are flagged by ASCAT, several wind vectors (most in strong wind variability conditions) are flagged by HSCAT-C, HSCAT-B, and OSCAT2.

B. Comparison with Buoy Winds

Four months of scatterometer winds are compared with the buoy winds, and the results are shown in Table 1. The scatterometer QC rejected winds are excluded in the statistics, which mainly represent Ku-band scatterometer cases with rain probability, usually associated with enhanced wind variability [17]. Nevertheless, the number of matchups for ASCAT is less than that for HSCAT or OSCAT, since the swath width of ASCAT is narrower. Because the HSCAT-C operates in inclined orbits, it provides relatively more times of measurements than HSCAT-B, OSCAT2, and ASCAT for latitudes between 74° N and 74° S. Thus, the number of matchups for HSCAT-C is the highest. Besides, several orbits of HSCAT-B in this period are unusable because of instrument anomaly or satellite maintenance.

As shown in Table 1, all scatterometer wind speeds show good agreements against buoy wind speeds, i.e., the SDs of wind speed differences range from 0.95 to 1.05 m/s. The wind speed biases of HSCAT-C, HSCAT-B, and OSCAT2 are all slightly negative. The SDs of meridional (v) wind component are also comparable among all scatterometers, while the SDs of zonal (u) wind component for ASCAT-B and ASCAT-C are slightly lower than that of HSCAT-C, HSCAT-B and OSCAT2. It is interesting to note that, the bias of u component for HSCAT-C, HSCAT-B and OSCAT2 are clearly larger than that of v component. This could be relevant to the wind retrieval algorithm, i.e., 2DVAR in wind ambiguity removal, and will also be discussed in section 3.3.

In the comparisons of wind direction, only the matchups for which the average wind speed of scatterometer and buoy is higher than 4 m/s are used. As a consequence, the wind direction RMSE shown in Table 1 may be sensitive to the scatterometer or buoy winds around 4 m/s. For instance, if the HSCAT-B (buoy) wind speeds are used as reference in condition sampling winds above 4 m/s, the resulting direction RMSE would be 16.1° (14.4°). Nevertheless, the wind direction RMSEs for these scatterometers are in a narrow range and comparable, i.e., between 14.8° and 16.0°.

C. Comparison with NWP Model Winds

The scatterometer winds are compared to the ECMWF forecast winds that are used in their wind retrieval processing, i.e., ECMWF operational stress-equivalent winds for ASCAT and OSCAT2, ECMWF operational real winds for HSCAT. The QC accepted winds are used in the calculation of bias and SD for wind speed, u component, and v component, whereas

TABLE 2
WIND COMPARISONS BETWEEN SCATTEROMETER AND NWP MODEL WINDS

SCATTEROMETER WINDS	QC RATIO	WIND SPEED		U COMPONENT		V COMPONENT		DIRECTION RMSE
		BIAS(M/S)	SD(M/S)	BIAS(M/S)	SD(M/S)	BIAS(M/S)	SD(M/S)	
HSCAT-C	6.1%	-0.04	1.12	-0.19	1.27	0.01	1.22	10.7°
HSCAT-B	6.2%	-0.03	1.11	-0.13	1.22	0.00	1.16	10.1°
OSCAT2	5.2%	-0.08	1.15	-0.11	1.27	-0.03	1.23	10.6°
ASCAT-B	0.4%	0.09	1.02	-0.06	1.22	-0.04	1.31	11.2°
ASCAT-C	0.4%	0.07	1.02	-0.05	1.21	-0.04	1.30	11.1°

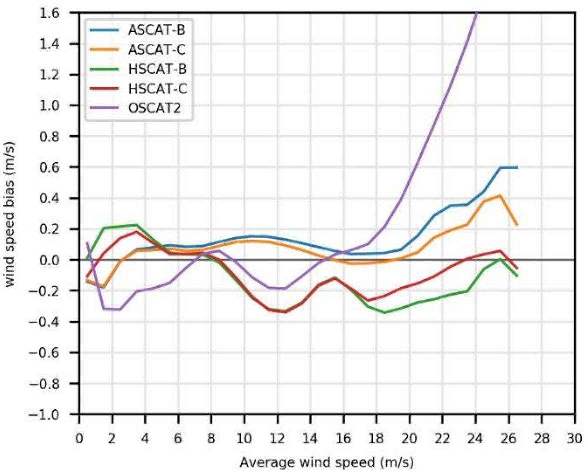

Fig. 2 Wind speed bias between scatterometers and NWP model winds as a function of average wind speed.

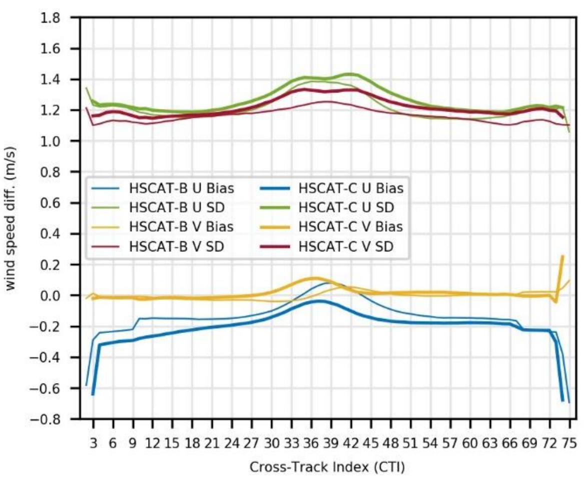

Fig. 3 Wind speed bias and SD between HSCAT-C (thick lines) or HSCAT-B and ECMWF real winds as a function of CTI for u and v components.

only the wind speeds (average) above 4 m/s are used in the calculation of wind direction RMSE. The results for all swath data are shown in Table 2, and as a function of wind speed are shown in Fig. 2, and as a function of cross-track index (CTI) are shown in Fig. 3. WVCs with the same CTI along the swath are measured by almost the same scatterometer geometries (i.e., antenna azimuths, incidence angles, and polarizations).

As shown in Table 2, about 6% of HSCAT-C or HSCAT-B data were flagged by QC, indicating the retrievals of these WVCs may have "poor" quality, whereas a very low fraction of winds is flagged in ASCAT wind products. In general, Table 2 shows consistent results with Table 1. The SDs of wind speed and wind components are comparable among all these scatterometers. The wind speed biases of HSCAT-C and HSCAT-B are slightly negative comparing to ECMWF real winds, but a larger negative bias is expected if comparing to ECMWF stress-equivalent winds. Stress-equivalent winds are on average ~0.2 m/s higher than real winds. However, figure 2 shows significant disparities of wind speed dependent biases among these scatterometers.

As we can see from Fig. 2, the behaviors of HSCAT-B and HSCAT-C are very similar, especially in the wind speed range of 4 to 17 m/s. The separations of wind speed biases above 17 m/s could be related to the differences in relative calibration or global sampling. This needs further investigation. The curves of ASCAT-B and ASCAT-C are also similar, and they show overlay biases for wind speed below 4 m/s and above 20 m/s, even if the identical instruments are in similar orbits at the same LST. Different from the others, the curve of OSCAT2 wind speed biases shows large negative biases at winds below 6 m/s and positive biases at winds above 18 m/s. Furthermore, similar oscillatory appears in wind speeds between 8 and 15 m/s, as compared to that of HSCAT-C or HSCAT-B. This may be related to GMF disparities between Ku and C band, that need further investigation [4].

Figure 3 shows wind speed bias and SD between HSCAT-C (thick lines) or HSCAT-B and ECMWF real winds as a function of CTI for u and v components. Biases of v component are almost zero and flat cross the swath, while biases of the u component are noticeable and show weak dependence on CTI. In fact, noticeable biases of u components are found in all these rotating-beam scatterometers, i.e., HSCAT-C, HSCAT-B, and OSCAT2, as also shown in Table 1 and 2. As is clearly seen in Fig. 3, the quality of the HSCAT winds varies against CTI. In the outer region of swath (CTI < 10 or CTI > 67), the bias and SD are relatively higher, mainly because only VV measurements and "poor" diversity of antenna looking azimuths are available. In addition, HSCAT data where CTI < 4 or CTI > 73 consist of partial orbits, where the sampling is restricted to high-latitude climate zones. Global ECMWF biases do depend on climate zone and hence varying ECMWF sampling may cause bias for these CTI [26, 27].

Based on the above results, small positive corrections are suggested to apply for the HSCAT-C and HSCAT-B backscatter measurements.

D. Comparison with Winds from other Scatterometers

Based on the collocated datasets, the HSCAT-C winds are compared with the HSCAT-B, OSCAT2, ASCAT-B, and ASCAT-C winds, separately. In the comparisons, if we only use

This article has been accepted for publication in a future issue of this journal, but has not been fully edited. Content may change prior to final publication. Citation information: DOI 10.1109/JSTARS.2021.3087742, IEEE Journal of Selected Topics in Applied Earth Observations and Remote Sensing

TABLE 3
WIND COMPARISONS BETWEEN HSCAT-C AND OTHER SCATTEROMETERS

Scatterometer winds	Data Ratio	Wind speed		Direction RMSE
		Bias(m/s)	SD(m/s)	
HSCAT-B	88.9%	0.03	0.56	10.5°
OSCAT2	90.5%	-0.00	0.66	11.5°
ASCAT-B	93.8%	-0.21	0.60	11.8°
ASCAT-C	93.5%	-0.19	0.60	11.7°

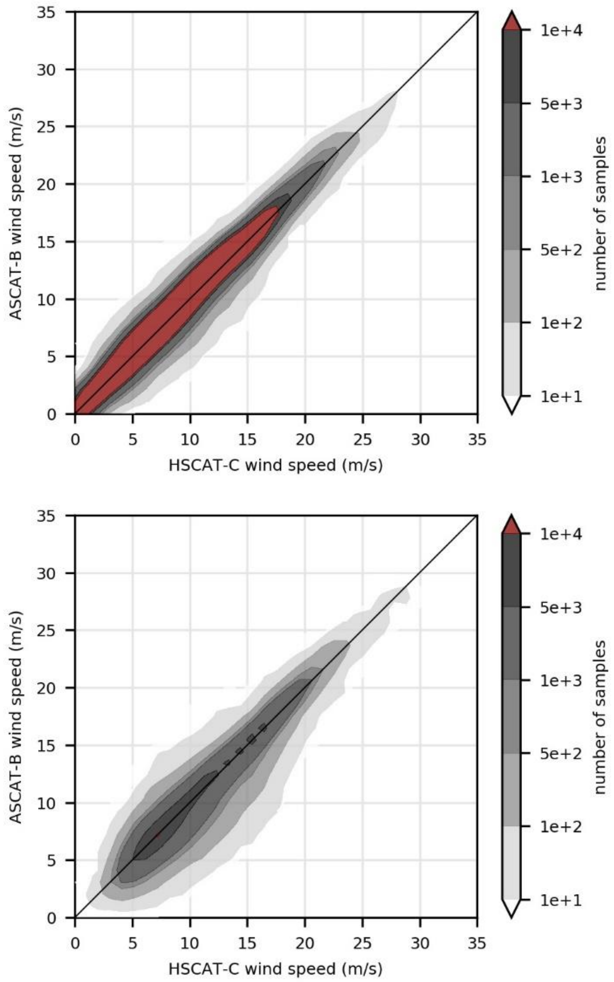

Fig. 4. Scatter plots for HSCAT-C wind speeds versus ASCAT-B wind speeds for the collocated winds that are (a): accepted by both QC; (b): HSCAT-C QC rejected, but ASCAT-B QC accepted.

the collocated winds that QC accepted by both sources, the results of wind speed biases and SDs, and direction RMSE are shown in Table 3. The column "data ratio" indicates the fraction of collocated winds accepted by both QC schemes. The SDs of wind speed differences for different collocations range from 0.56 to 0.66 m/s. Since all scatterometer winds have 25-km size Wind Vector Cells, their spatial representations are comparable. Thus the SDs of wind speed differences are much smaller than that of scatterometer versus buoy or NWP winds. We note that HSCAT-C winds show the best agreements with HSCAT-B winds, which may be due to global sampling, instrument characteristics and/or calibration and processing settings (e.g., QC or ambiguity removal).

Figure 4a gives the scatter plot for the category of collocated and QC-accepted HSCAT-C and ASCAT-B winds, while Figure 4b gives the scatter plot for the category of collocated winds that ASCAT-B QC accepted, but HSCAT-C rejected. The percentage of the collocated winds that ASCAT-B QC accepted, but HSCAT-C QC rejected is about 5.4%. The corresponding wind speed bias and SD are 0.12 m/s and 1.33 m/s respectively, and the wind direction RMSE is 24.0°. Thus, the overall quality of these QC-rejected winds is much worse than of the QC-accepted winds. However, a large number of data appear along the diagonal in Fig. 4b, indicating that a number of HSCAT-C winds are false alarmed by its QC procedure. We first note that both Ku-band QC is active due to wind variability in rainy areas. This partly explains the relatively high SD for the QC-rejected winds, as increased wind variability, violates the assumption of NRCS homogeneity generally used in radar and increases (disperses) the relative differences between the different geometrical views in a WVC, increasing retrieval noise. Furthermore, wind variability increases the collocation error, as both temporal and spatial differences will much affect the comparisons in increased variability conditions. We also note that increased variability conditions are of the largest meteorological interest generally, hence rejecting those appears rather detrimental. When rain does appear in an ocean area that is measured by both HSCAT-C and ASCAT-B, then the wind-induced radar backscatter measurements received by the C-band ASCAT-B may be negligibly contaminated, while that received by the Ku-band HSCAT-C should be considerably contaminated [17]. Besides, only a very small amount of data in this category appear in low (< 4 m/s) wind speed conditions.

E. Spectral Analysis

The spectra of scatterometer winds for u and v wind components are shown in Fig. 5. Given their similar instrument and processing, HSCAT and OSCAT2 should show rather similar spectra. However, the spectral content of both HSCAT-B and -C appears somewhat lower than that of OSCAT2. This may be due to differences in spatial footprint processing, noise properties and calibration. For the latter we refer to the bias dispersion in Fig. 2 for OSCAT2, which may affect the perceived spatial variability by the spectral analysis in Fig. 5. This can obviously be circumvented by a more elaborate calibration effort on OSCAT2, which is ongoing.

The spectra require long samples and are hence affected by QC properties, which cause sample gaps. In particular, Ku-band scatterometers may relatively more often sample stable flow areas (without enhanced wind variability causing QC gaps) with relatively low spectral content, displacing the amplitude spectra downward with respect to ASCAT. A way to solve such disparity would be to perform spatial variance analyses of collocated data sets [28].

IV. Conclusions

With the in-orbit operation of the Chinese Ku-band HSCAT-C scatterometer, the sea surface wind measurements provided

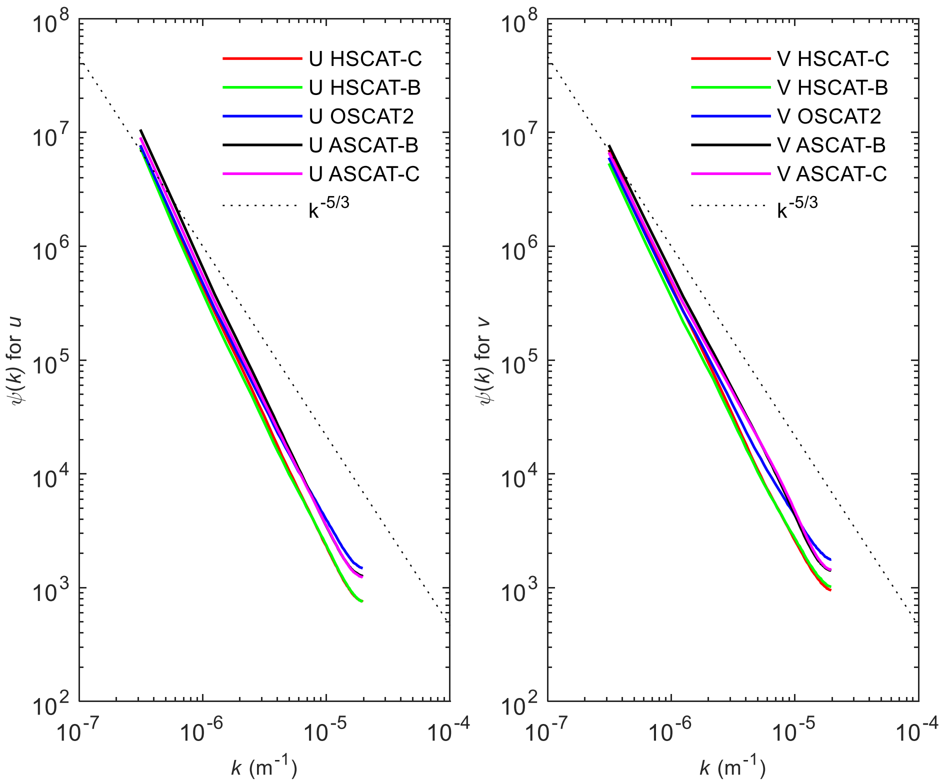

Fig. 5. Spectra of the scatterometer winds for (a) u wind component and (b) v wind component.

by space-borne scatterometers over the global oceans are significantly enhanced in terms of coverage, revisit time intervals and collocation opportunity. In this study, the HSCAT-C wind product are validated and the error characteristics are shown and discussed in the context of collocations with the wind products from ASCAT-B, ASCAT-C, OSCAT2 are also involved.

The overall performance of the HSCAT-C wind product is very good. In comparison with buoy winds, the wind speed SD and direction RMSE are 1.03 m/s and 15.9° respectively. The HSCAT-C winds show very good agreements with the HSCAT-B winds, especially in the range of [4, 17] m/s. In comparison with HSCAT-B winds, the results show that the overall wind speed bias and SD are 0.02 m/s and 0.55 m/s respectively, along with wind direction RMSE 10.7°. Even though, there is still room for further improving the consistencies of wind products from HSCAT-C and HSCAT-B. As HSCAT-C is a rotating pencil-beam scatterometer, some common error characteristics are also clearly found in its wind products. The quality of the winds varies across the swath, and it is relatively worse in the nadir and outer regions of the swath. The further inter-calibration of HSCAT-C and HSCAT-B backscatter measurements and wind products are strongly recommended suggestions for further study.

Moreover, the HSCAT-C wind speed dependence on sea surface temperature (SST) is not shown in this study, but the SST effects have been well demonstrated in our previous work, and again an SST extended GMF is necessarily needed in Ku-band scatterometer wind processing. Using the special orbit of the HSCAT-C, an SST-dependent GMF for HSCAT scatterometers can be verified, following the NSCAT-5 made for the RapidScat which was mounted on the international space station. The intercalibration with C-band scatterometers and radiometers furthermore fits in this context, linking these instrument performances to both in-situ and NWP model data using TC tools.

ACKNOWLEDGMENT

The authors are grateful to ISRO ((Indian Space Research Organization)) for the mission data of SCATSAT-1/OSCAT2, to ECMWF for providing model and buoy data.

REFERENCES

[1] Y. Zhang, B. Mu, M. Lin and Q. Song, “An evaluation of the Chinese HY-2B satellite's microwave scatterometer instrument”, *IEEE Trans.Geosci. Remote Sens.*, DOI: 10.1109/TGRS.2020.3008405.

[2] A. Stoffelen, R. Kumar, J. Zou, V. Karaev, P.S. Chang, E. Rodriguez, “Ocean surface vector wind observations”, Remote Sensing of the Asian Seas. Springer, Cham, https://doi.org/10.1007/978-3-319-94067-0_24, Print ISBN 978-3-319-94065-6, Online ISBN 978-3-319-94067-0.

[3] H. Wang, J. Zhu, M. Lin, Y. Zhang and Y. Chang, “Evaluating Chinese HY-2B HSCAT ocean wind products using buoys and other scatterometers”, *IEEE Geoscience and Remote Sensing Letters*, 17(6), pp.923-927, 2019.

[4] Z. Wang, A. Stoffelen, B. Zhang, Y. He, W. Lin and X. Li, “Inconsistencies in scatterometer wind products based on ASCAT and OSCAT-2 collocations”, *Remote Sensing of Environment*, 225, pp.207-216, 2019.

[5] S.A. Bhowmick, J. Cotton, A. Fore, R. Kumar, C. Payan, E. Rodríguez, A. Sharma, B. Stiles, A. Stoffelen and A. Verhoef, “An assessment of the performance of ISRO’s SCATSAT-1 Scatterometer”, Curr. Sci, 117(6), pp.959-972, 2019.

[6] W. Lin, M. Portabella, A. Stoffelen, J. Vogelzang and A. Verhoef, “ASCAT wind quality under high subcell wind variability conditions”, *Journal of Geophysical Research: Oceans*, 120(8), pp.5804-5819, 2015.

[7] A. Verhoef, J. Vogelzang, J. Verspeek and A. Stoffelen, "Long-term scatterometer wind climate data records", *IEEE Journal of Selected Topics in Applied Earth Observations and Remote Sensing*, 10(5), pp.2186-2194, 2017.
[8] B.W. Stiles, B.D. Pollard and R.S. Dunbar, "Direction interval retrieval with thresholded nudging: A method for improving the accuracy of QuikSCAT winds", *IEEE Trans.Geosci. Remote Sens.*, 40(1), pp.79-89, 2002.
[9] Z. Wang, A. Stoffelen, J. Zou, W. Lin, A. Verhoef, Y. Zhang, Y. He and M. Lin, "Validation of new sea surface wind products from Scatterometers Onboard the HY-2B and MetOp-C satellites", *IEEE Trans.Geosci. Remote Sens.*, 58(6), pp.4387-4394, 2020.
[10] A. Bentamy, S.A. Grodsky, J.A. Carton, D. Croizé-Fillon and B. Chapron, "Matching ASCAT and QuikSCAT winds", *Journal of Geophysical Research: Oceans*, 117(C2), 2012.
[11] Z. Wang, A. Stoffelen, C. Zhao, J. Vogelzang, A. Verhoef, J. Verspeek, M. Lin and G. Chen. "An SST-dependent Ku-band geophysical model function for RapidScat", *Journal of Geophysical Research: Oceans*, 122(4), pp.3461-3480, 2017.
[12] M. Zheng, X.M. Li and J. Sha, "Comparison of sea surface wind field measured by HY-2A scatterometer and WindSat in global oceans", *Journal of Oceanology and Limnology*, 37(1), pp.38-46, 2019.
[13] J. Yang and J. Zhang, "Comparison of Oceansat-2 scatterometer wind data with global moored buoys and ASCAT observation", *Advances in Meteorology*, 2019.
[14] A. Stoffelen, "Toward the true near-surface wind speed: Error modeling and calibration using triple collocation", *Journal of geophysical research: oceans*, 103(C4), pp.7755-7766, 1998.
[15] J. Vogelzang, A. Stoffelen, A. Verhoef and J. Figa-Saldaña, "On the quality of high-resolution scatterometer winds", *Journal of Geophysical Research: Oceans*, 116(C10), 2011.
[16] A. Chakraborty, R. Kumar and A. Stoffelen, "Validation of ocean surface winds from the OCEANSAT-2 scatterometer using triple collocation", *Remote Sensing Letters*, 4(1), pp.84-93, 2013.
[17] X. Xu and A. Stoffelen, "Improved rain screening for Ku-Band wind scatterometry", *IEEE Transactions on Geoscience and Remote Sensing*, vol. 58, no. 4, pp. 2494-2503, April 2020, doi: 10.1109/TGRS.2019.2951726, 2019.
[18] J. Vogelzang and A. Stoffelen, "Quadruple collocation analysis of in-situ, scatterometer, and NWP winds", Earth and Space Science Open Archive, https://doi.org/10.1002/essoar.10505872.1, 2021.
[19] J. De Kloe, A. Stoffelen, A. Verhoef, "Improved use of scatterometer measurements by using stress-equivalent reference winds", *IEEE J. Sel. Top. Appl. Earth Obs. Remote Sens.* 10 (5). https://doi.org/10.1109/JSTARS.2017.2685242, 2017.
[20] OSI SAF, "ScatSat-1 wind product user manual", SAF/OSI/CDOP2/KNMI/TEC/MA/287, version 1.3, 2018. Available online: https://scatterometer.knmi.nl/publications/pdf/osisaf_cdop2_ss3_pum_scatsat1_winds.pdf (Accessed on Feb 10, 2020).
[21] OSI SAF, "ASCAT wind product user manual", SAF/OSI/CDOP/KNMI/TEC/MA/126, version 1.16, 2019. Available online: https://scatterometer.knmi.nl/publications/pdf/ASCAT_Product_Manual.pdf (Accessed on Feb 10, 2020).
[22] J.R. Bidlot, D.J. Holmes, P.A. Wittmann, R. Lalbeharry and H.S. Chen, "Intercomparison of the performance of operational ocean wave forecasting systems with buoy data," Wea. Forecasting, vol. 17, no. 2, pp. 287–310, Apr. 2002.
[23] W.T, Liu, K.B. Katsaros and J.A. Businger, "Bulk parameterization of air-sea exchanges of heat and water vapor including the molecular constraints at the interface," *J. Atmos. Sci.*, vol. 36, no. 9, pp. 1722–1735, Sep. 1979.
[24] T. Kilpatrick, S.P. Xie, H. Tokinaga, D. Long and N. Hutchings, "Systematic scatterometer wind errors near coastal mountains", Earth and Space Science, 6(10), pp.1900-1914, 2019.
[25] N. Hutchings, T. Kilpatrick and D.G. Long, "Ultrahigh resolution scatterometer winds near Hawaii", Remote Sensing, 12(3), p.564, 2020.
[26] M.B. Rivas and A. Stoffelen, "Characterizing ERA-Interim and ERA5 surface wind biases using ASCAT", *Ocean Sci.*, 15, 831–852, https://doi.org/10.5194/os-15-831-2019, 2019.
[27] A. Trindade, M. Portabella, A. Stoffelen, W. Lin and A. Verhoef, "ERAstar: A high-resolution ocean forcing product," *IEEE Trans. Geosci. Remote Sens.*, vol. 58, no. 2, pp. 1337-1347, Feb. 2020, doi: 10.1109/TGRS.2019.2946019, 2020.
[28] J. Vogelzang, G.P. King and A. Stoffelen, "Spatial variances of wind fields and their relation to second-order structure functions and spectra", *J. Geophys. Res. Oceans*, 120, 1048–1064, doi:10.1002/2014JC010239, 2015.

Zhixiong Wang (Member, IEEE) was born in Shaanxi, China, in 1987. He received the master's degree in photogrammetry and remote sensing and the Ph.D. degree in ocean detection technology from the Ocean University of China, Qingdao, China, in 2014 and 2017, respectively.

From 2015 to 2016, he was a joint Ph.D. Student with the Royal Netherlands Meteorological Institute, De Bilt, The Netherlands, with funding from the China Scholarship Council. Since July 2017, he has been a member of the Laboratory for Regional Oceanography and Numerical Modeling, Qingdao National Laboratory for Marine Science and Technology, Qingdao. He is currently a Faculty Member with the Nanjing University of Information Science and Technology (NUIST), Nanjing, China, focusing on microwave remote sensing and marine physics.

Juhong Zou received the Ph.D. degree from the Chinese Academy of Sciences, Shanghai, China, in 2009.

In 2011, he was responsible for the development of ocean wind retrieval algorithms of HY-2A satellite microwave scatterometer. He is currently the Deputy Chief Designer of the HY-2B/C satellite ground data processing systems with National Satellite Ocean Application Service, Beijing, China. His research interests include microwave scatterometer ground based data processing, ocean wind retrieval, and oceanographic applications of satellite remote sensing.

Ad Stoffelen (Senior Member, IEEE) was born in 1962 in the Netherlands. He received the M.Sc. degree in physics from the Technical University of Eindhoven, Eindhoven, The Netherlands, in 1987, and the Ph.D. degree in meteorology on scatterometry from the University of Utrecht, Utrecht, The Netherlands.

Currently, he leads a group on active satellite sensing in Royal Netherlands Meteorological Institute, De Bilt, The Netherlands, and is involved in topics from future missions and retrieval to 24/7 operations, user training and services. He is also deeply involved in the European Space Agency ADM-Aeolus Doppler Wind Lidar mission.

Wenming Lin (Senior Member, IEEE) was born in Fujian, China, in 1984. He received the B.Sc. degree in engineering from Wuhan University, Wuhan, China, in 2006, and the Ph.D. degree in engineering from the National Space Science Center, Chinese Academy of Sciences, Beijing, China, in 2011.

From 2011 to 2017, he was a Post-Doctoral Researcher at the Institut de Ciències del Mar, Barcelona, Spain, focusing on the advanced oceanographic data processing methods, remote sensing of ocean-surface winds, and data assimilation. He is currently a Faculty Member with the Nanjing University of Information Science and Technology, Nanjing, China, focusing on ocean remote sensing.

Anton Verhoef was born in 1964 in the Netherlands. He received the M.Sc. degree in physics in 1989, and the Ph.D. in solid state physics in 1994, both from the Rijksuniversiteit Groningen, Groningen, The Netherlands.

He is currently with the Royal Netherlands Meteorological Institute, De Bilt, The Netherlands, and working on scatterometry processing software development, data validation, quality monitoring, and user services.

Xiuzhong Li was born in Shandong, China, in 1985. He received the M.S. degree in physical oceanography from the First Institute of Oceanography, Ministry of Natural Resources, Qingdao, China, in 2011, and the Ph.D. degree in atmospheric remote sensing science and technology from the Nanjing University of Information Science and Technology, Nanjing, China, in 2016.

He is a Faculty Member with the Nanjing University of Information Science and Technology, where he is working on ocean wave and wind vector remote sensing.

Yijun He (Member, IEEE) received the B.S. degree in physics from Hunan Normal University, Changsha, China, in 1985, the M.S. degree in applied physics from Xidian University, Xi'an, China, in 1990, and the Ph.D. degree in microwave theory and technology from Southeast University, Nanjing, China, in 1993.

He was with the Key Laboratory of Ocean Circulation and Waves, Institute of Oceanology, Chinese Academy of Sciences, Qingdao, China, where he was the Head of the Remote Sensing Group and the Senior Scientist of satellite oceanography from 1996 to 2011. He was a Post-Doctoral Fellow with Ocean Remote Sensing Institute, Ocean University of China, Qingdao, from 1993 to 1996. He was a Visiting Scientist with the University of Hamburg, Hamburg, Germany, the Bedford Institute of Oceanography, Dartmouth, NS, Canada, and the University of Delaware, Newark, DE, USA. He is a Professor of ocean remote sensing and the Dean of the School of Marine Sciences, Nanjing University of Information Science and Technology, Nanjing, China. His research interests include ocean waves, sea-surface wind speed, and other ocean-surface features related to remote sensing by full polarization synthetic aperture radar and other microwave radar at low incidence angle, air-sea gas exchange using microwave remote sensing and numerical models, sea-surface scattering of electromagnetic waves, and mesoscale and submesoscale ocean dynamics.

Youguang Zhang was born in Shandong, China, in 1971. He received the Ph.D. degree in oceanography from the Institute of Oceanology, Chinese Academy of Sciences, Qingdao, China, in 2004.

He was with the National Satellite Ocean Application Service (NSOAS), State Oceanic Administration, Beijing, China, since 2004, where he is currently a Researcher and the Departmental Director. He is also the deputy chief engineer of ground application system for HY-2 satellite. He has hosted and taken part in more than 30 projects, such as Manned Flight Project, Marine Public, 863 Project, and National Research and Development Plan. He has authored or co-authored more than 50 papers. His research interests include the microwave remote sensing of the ocean, data processing, and the calibration of active microwave remote sensors, satellite ground application system construction, and the advanced research of new type ocean remote sensing payloads.

Mingsen Lin received the Ph.D. degree in computing mathematics from the Computing Center, Chinese Academy of Sciences, Beijing, China, in 1992.

He was a Deputy Chief Designer of ground application system for HY-1 and HY-2 satellites, where he organized the argument of Chinese Ocean Satellite outline, and managed the construction of ground application system for Chinese Ocean Satellite with National Satellite Ocean Application Service, Beijing. He is the Founder of satellite ocean remote sensing in China. He plays an important role in the development of Chinese Ocean Satellite and Manned Space Flight. His research interests include remote sensing of the ocean and computation fluid dynamics.